Polym. Bull. (2018) 75:2053–2069
https://doi.org/10.1007/s00289-017-2146-4

ORIGINAL PAPER

Incorporation of CuO nanoparticles into thin-film composite reverse osmosis membranes (TFC-RO) for antibiofouling properties

A. García[1] · B. Rodríguez[1] · D. Oztürk[1] · M. Rosales[1,2] · D. I. Diaz[3] · A. Mautner[4]

Received: 24 May 2017 / Revised: 25 July 2017 / Accepted: 31 July 2017 /
Published online: 3 August 2017

Abstract The effect of the incorporation during the interfacial polymerization process of copper-oxide (CuO) nanoparticles in thin-film composite (TFC) reverse osmosis (RO) membrane on their antibiofouling and desalinization performance have been studied. Membranes were characterized by fourier transform infrared spectroscopy (FTIR), scanning electron microscopy (SEM), energy-dispersive X-ray spectroscopy (EDX), atomic force microscopy (AFM), zeta potential and contact angle measurements. Bactericidal tests were performed using *Escherichia coli* and anti-adhesion properties were confirmed by fluorescence microscopy. Membrane performance using a cross flow cell was evaluated. XRD and SEM–EDX analyses confirmed the incorporation of these nanoparticles into the membrane. Similar contact angle, higher surface roughness and less negatively charged surface on modified membrane compared to that of the pristine membrane were observed. However, an excellent anti-adhesion and bactericidal effect were observed, mainly attributed to the copper toxicity. The desalination performance of the modified membrane showed an important salt rejection with stable water flux. In conclusion, the incorporation of CuO nanoparticles into TFC-RO membranes during the interfacial polymerization process is a potential alternative method to improve the antibiofouling capacities without impairing the performance of the membrane.

✉ A. García
andreina.garcia@amtc.cl

[1] Advanced Mining Technology Center (AMTC), Universidad de Chile, 8370451 Santiago, Chile

[2] Nanoscale Functional Materials Laboratory, Department of Materials Science, Universidad de Chile, Beauchef 851, Santiago, Chile

[3] Instituto de Física, Pontificia Universidad Católica de Chile, 7820436 Santiago, Chile

[4] Polymer and Composite Engineering (PaCE) Group, Institute of Materials Chemistry and Research, University of Vienna, 1090 Vienna, Austria

Keywords TFC membrane · Reverses osmosis · CuO nanoparticle · Antibiofouling · Desalination

Introduction

Membrane-based processes represent the main technology for desalination processes, including reverses osmosis (RO), forward osmosis (FO), ultrafiltration (UF), microfiltration (MF), nanofiltration (NF) and membrane distillation (MD) processes [1–4].

In the case of reverse osmosis (RO), the most known polymer membranes have been made from polymers with aromatic polyamide groups (TFC) which dominate RO membrane field nowadays by their good capacities (water flux and solute rejection), but they are not completely resistant to fouling [1, 2, 5].

Membrane fouling is considered an inevitable obstacle affecting seawater desalination plants causing a decrease in membrane performance, which consequently increases the operational and maintenance costs [1, 2]. It can be broadly categorized into inorganic fouling, organic fouling and biofouling [1, 5].

Biofouling is caused by the attachment and proliferation of microorganism communities which eventually form a biopolymer matrix, considered a biofilm, over the membrane surface [5]. Hence, a new generation of membranes with inherent antibiofouling capabilities needs to developed. Moreover, innovative methods to develop them without affecting their desalination performance and other properties are also needed.

In the search to improve the antibiofouling capabilities of these membranes, the incorporation of inorganic particles with antimicrobial properties into membranes has been reported [1, 6–9]. Several studies have shown that Ag and TiO_2 nanoparticles show good antibiofouling properties and can be used for the development of hybrid organic/inorganic RO membranes [1, 7–9]. In the same way, the incorporation of copper should also be investigated, as these also show antimicrobial properties.

The germicidal properties of copper make it suitable for incorporation into several antibiofouling polymeric materials [10–12]. Both copper ions and nanoparticles have been proposed to modify membranes in order to improve their properties mainly the antibiofouling effect.

For example, the immobilization of Cu ions on UF and RO membrane surfaces has shown the improvement of antibacterial properties [13–16]. Moreover, Cu particles have also been reported in membrane technologies as ultrafiltration and nanofiltration membranes [17, 18].

In the case of RO membranes, different ways for modification with Cu particles have also been reported, e.g., the modification of commercial RO membranes with copper hydroxide ($Cu(OH)_2$) particles adsorbed [19]. Furthermore, polyamide (PA) functionalization with Cu-nanoparticles (Cu-NPs) was used to cover a pristine TFC membrane by dip-coating [20]. Recently, in situ surface functionalization with Cu-NPs on the surface of TFC membrane was also developed [21]. And finally, in

another recently proposed application, vacuum membrane distillation (MD) was modified by incorporating CuO nanoparticles using phase inversion methods [22].

Owing to the above-mentioned facts, Cu particles and nanoparticles have been used for modifying UF, NF and commercial RO membranes, in order to enhance their antibiofouling properties. However, to our knowledge there are no previous reports on the incorporation of CuO nanoparticles within polyamide layer of TFC-RO membranes during the interfacial process polymerization.

CuO nanoparticles are a promising material in membrane applications given that it is a highly ionic metal oxide, cheaper than Ag, can be mixed readily with polymers and exhibits relatively stable chemical and physical properties. Additionally, it shows exceptionally good antimicrobial properties against a wide variety of bacteria, fungi and microalgae [23–26].

Hence, this study presents an alternative method for enhancing the antibiofouling properties of TFC membranes through the incorporation of CuO nanoparticles into the polyamide layer of this membrane during the interfacial polymerization process. Modified membrane was characterized to confirm the incorporation of nanoparticles into the membrane and evaluate the changes in the surface properties. Moreover, antibiofouling effect was analyzed through bactericidal and anti-adhesion tests. Finally, desalination performance (flux and salt rejection) were evaluated in order to confirm that the incorporation of CuO nanoparticles into membranes improves the antibiofouling capacities without impairing the performance of the membrane.

Materials and experimental methods

Materials

The polysulfone Udel P-3500 MB7 (in pellet form; Solvay Advanced Polymers, molecular weight 83,000 g/mol, 1-methyl-2-pyrrolidinone (NMP, >99.5%, Sigma Aldrich) and *N*,*N*-dimethylformamide (DMF, >99%, Sigma Aldrich) were used to fabricate the PSL sample used as the support. Commercial CuO nanoparticles (< 50 nm) were obtained from Sigma Aldrich. *m*-Phenylenediamine (MPD) and trimesoyl chloride (TMC), which were used as the monomers for polyamide (PA), were obtained from Sigma Aldrich. Finally, NaOH (>97%) and *n*-hexane (>95%) were obtained from Sigma Aldrich.

Preparation of PSf supports

The PSf support was fabricated using the phase-inversion method [17, 27]. A casting PSf solution in a DMF/NMP mixture (4:1) was kept agitated for 2 h at 50 °C, to allow for complete dissolution. The composition of the PSf/(DMF/NMP) solution was 15/85 (wt %).

The PSf support was prepared by casting the polymer solutions uniformly on glass plate using a casting knife with a knife gap set at 200 μm. Next, the support was recovered from the coagulation bath for 1 min and washed thoroughly with distilled water to remove any residual solvent. The entire casting set up was kept in

an air-conditioned room with the temperature being controlled at 25 °C and the relative humidity at 20% during the entire PSf casting process.

Preparation of unmodified and modified membranes

The TFC-RO membrane was synthesized by an interfacial polymerization reaction of the aqueous phase of MPD and the organic phase of TMC on the porous PSf substrate. The PSf support was placed for 2 min in a 2 wt% aqueous MPD solution containing 0.05 wt% sodium hydroxide (NaOH). The excess MPD solution remaining on its surface was removed with Kimwipes wipers. Next, the membrane was immersed in a 0.2 wt% TMC solution in hexane for 1 min to allow interfacial polymerization. This resulted in the formation of a thin film of PA on the surface of the PSf support. The resulting membrane was subsequently cured in an air-circulation oven at 75 °C for 8 min. Finally, the membrane was washed with distilled water and dried at room temperature for 24 h [27].

The modified membrane was prepared as follows: CuO nanoparticles (1.0 wt%) were homogeneously dispersed in an MPD solution using ultrasonic vibration to prepare nanoparticle-entrapping PA layers on the porous PSf supports, referred to as (PA-CuO)/PSf.

Characterization of membranes

The presence of CuO in the membranes was confirmed using X-ray diffraction (XRD) analyses (Bruker, D8 Advance, $CuK_{\alpha 1}$, 40 kV/30 mA); the patterns were measured for 2θ values of 0°–90°. Attenuated total reflectance Fourier transform infrared spectroscopy (ATR-FTIR) (Model iS10, Nicolet) was used to identify the functional groups in the dense PA layers of the membranes. The morphologies of the membranes (cross-sectional and surface) were studied using scanning electron microscopy (SEM) (INSPECT F-50, FEI Co.). The membranes were then sputter-coated with a thin film of carbon to make them conductive. The membranes were snapped under liquid nitrogen to give a generally consistent and clean cut. Subsequently, membranes were investigated using atomic force microscopy (AFM) in an AFM/STM Omicron Nanotechnology model SPM1 in contact mode with a tip of silicon. The dimension of the cantilever was 450 μm long and 50 μm wide. The microscopies were taken in three different zones for each sample and three measurements in each zone were realized. Surface roughness (RMS) of samples was calculated using WSxM software over $2500 \times 2500\ nm^2$ images. Elemental analyses were performed using energy-dispersive X-ray spectroscopy (EDS) (Model APOLLO-X, EDAX, software Genesis V6.33), in order to further confirm the presence of the CuO nanoparticles within the membranes. The changes in hydrophilicity of membranes were studied by contact angle measurements. Contact angles were measured by placing a sessile drop using 5 μL of ultra-pure water on the membrane and performing drop-shape analysis. Contact angle images were captured using a Digi-Microscope camera, a zoom lens of 500X and a resolution of 11 μm/pixel. Captured images were analyzed with the imaging processing software ImageJ. Three images were recorded per drop on a membrane and averaged. The

determination of the zeta potential (ζ-potential) of the membranes was performed with a SurPASS electrokinetic analyzer from Anton Paar (Graz, Austria) as a function of pH in an adjustable gap cell (gap width 100 μm). The electrolyte solution (1 mM KCl) was pumped through the cell while steadily increasing the pressure to 300 mbar. The pH was controlled by titrating 0.05 mol L^{-1} KOH and 0.05 mol L^{-1} HCl into the electrolyte solution. For each sample type one measurement with two specimens sized 10 × 20 mm was performed. For the calculation of the ζ-potential the measured streaming current was used.

Antibiofouling tests

Bactericidal test

The bactericidal properties of the unmodified and modified membranes were evaluated by colony-forming unit method using *Escherichia coli* (*E. coli*) as model gram-negative bacteria. Bacteria were first cultured in tryptone soya broth (TSB) solution (30 g/L) and incubated in a shaking incubator in 200 rpm at 30 °C overnight. Then the bacteria solution was centrifuged at 3000 rpm for 10 min to remove the nutrients and washed in phosphate-buffered saline (PBS). This procedure was repeated three times to ensure all nutrients were removed. The prepared bacteria were diluted 100 times in PBS to obtain a bacterial concentration about 1×10^7 cell/mL. The membrane samples which were cut into the squares of 2×2 cm^2 and sterilized by ultraviolet radiation for 30 min, immersed separately into the 10 mL prepared bacteria solution. Bacteria suspensions with membranes were incubated in the shaking incubator at 30 °C for 4 h. At the same time, 10 mL bacteria solution without membrane incubated as a control. After that, the treated solutions were serially diluted with PBS. From the highest dilution, 50 μL of the solution was pipetted into LB agar plates and then spread over the entire surface. The agar plates were incubated at 35 °C overnight and were observed for colonies developed to estimate the number of viable *E. coli* remained in the suspensions.

Anti-adhesion test

The degrees of attachment of bacteria to the membrane surfaces were assessed with *E. coli* as well. The bacteria were prepared in the same manner as the bactericidal tests. Three pieces of each type of membrane (unmodified and modified membrane) with an area of 2 cm^2 were incubated in the bacterial suspension at 30°C while being shaken at 200 RPM. After being incubated for 4 h, the membranes were removed from the suspension and gently rinsed with a 0.85 wt% NaCl solution in water. Two types of staining cell on the membranes were performed. First, for staining total cells on the membranes, they were stained with 1 μg/mL 4′,6-diamidina-2-phenylidole. On the other hand, for staining live and dead cells on the surface of membranes, they were rinsed with LIVE/DEAD BacLightTM Bacterial Viability Kit. Equal amounts (1.5 μL/mL) of SYTO 9 and SYTO PI (propidium iodide) dyes were diluted in 1 mL of a 0.85 wt% NaCl solution. Dyes were added to the top surface of the membrane and incubated for 15 min in the dark. After

incubation, the stained cells were observed under the epifluorescence microscope (Zeiss, AxioLab A1, Germany) with a 100× objective. The total and live/dead cell counts were determined and used to calculate the cell densities.

Desalination performance test

Membranes' performance was evaluated in terms of the permeate flux and salt rejection by using a cross flow test cell with an effective area of 33 cm^2 and a feed solution of 1000 mg/L NaCl at 300 psi, following previous report [28].

The permeate flux test of membranes during 60 min was calculated by Eq. (1) [29]:

$$J = V/A \times \Delta t, \tag{1}$$

where J (L m^{-2} h^{-1}) is the membrane flux, V (L) is the volume of permeated water, A (m^2) is the membrane area and Δt (h) is the permeation time. The experiments were carried out at a temperature of 25 ± 1 °C.

Additionally, solute rejection was measured from the feed and permeate solution concentrations by Eq. (2) [30]:

$$\text{Rejection } (\%) = (C_f - C_p/C_f) \times 100, \tag{2}$$

where C_f and C_p are the concentrations of the feed solution and permeate solution, respectively. The conductivity of these two solutions was measured to obtain their respective concentration values.

Results and discussion

Analysis of surfaces and morphologies of membranes

XRD patterns of various membranes are shown in Fig. 1, along with that of the CuO nanoparticles. XRD pattern for CuO nanoparticles exhibits two main peaks, at 35.5° and 38.7°, which correspond to the reflections from the (−1 1 1) and (2 0 0) planes. These matched well with the monoclinic phase of CuO [31], as well as with those reported for CuO in the literature. Further, after the CuO nanoparticles had been incorporated into the PA layer to form modified membranes (PA-CuO)/PSf), there were no changes in their XRD pattern. This indicated that no crystal-phase transitions occurred during the incorporation of the CuO nanoparticles in the membranes.

Infrared (IR) spectroscopy was performed to study the characteristic functional groups present in the various membranes. Figure 2 shows the IR spectra of the unmodified membrane (PA/PSf) and the modified membrane ((PA-CuO)/PSf). The IR spectra of the unmodified and modified membranes exhibited weak peaks at approximately 1610 and 1680 cm^{-1}; these were assignable to amide bands [32, 33]. The band at ~1610 cm^{-1} is characteristic of the PA aromatic ring while the band at ~1680 cm^{-1} corresponded to the C=O stretching vibration of PA. In addition,

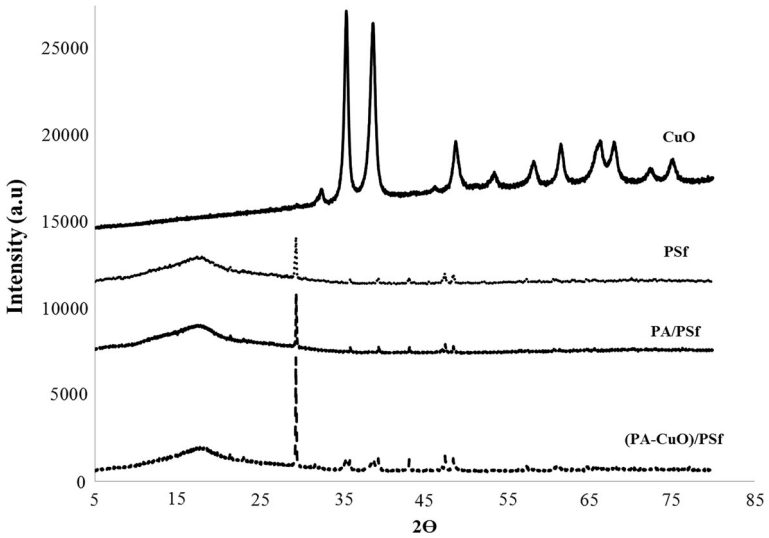

Fig. 1 XRD patterns of the samples

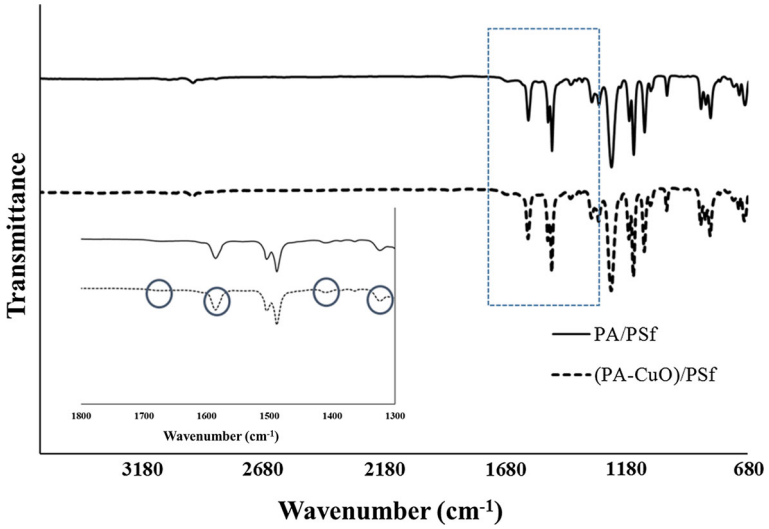

Fig. 2 ATR-FTIR spectra of the membranes

peaks were observed at 1406 and 1339 cm^{-1}; these corresponded to the stretching vibrations of the –(C–N)– and –(C–O)– bonds in the polymer chain, respectively [34]. One peak observed at 2959 cm^{-1} could be assigned to aliphatic CH stretching [33].

Thus, it was confirmed that PA layers were formed successfully on the PSf support, via interfacial polymerization. These results verified that the incorporation

of the CuO nanoparticles did not affect the formation of PA layers on the PSf support, a structure that is characteristic of TFC membranes.

Figure 3 shows a FE-SEM image of the surface of the (PA-CuO)/PSf membrane. It can be noted that the morphology of the membrane surfaces corresponded to so-called ridge-and-valley structure [35]. Moreover, the membrane surface reveals a tightly packed globular structure and protuberances. The development of these protuberances is so prominent as to produce the strands of polymer, which in turn form the ridges and valleys. Similar results have been reported for polyamide membranes synthesized with MPD/TMC [36].

Moreover, EDX analyses of the surfaces of (PA-CuO)/PSf membrane is shown in Fig. 4. The table (inset) presents the results of quantitative analyses, indicating that C, N, O and Cu were the main elements on the membrane surfaces. These results confirmed the presence of CuO nanoparticles in the PA layers of membranes.

Figure 5a, b shows SEM image of the cross-section of unmodified and modified membranes, respectively. The formation of an ultrathin layer of PA over the PSf support can be seen clearly in both cases. CuO nanoparticles (bright spots) can be lightly seen on the top of the modified membrane in comparison with unmodified membrane, indicating their incorporation into the dense PA layer. On the other hand, it can be seen that the PSL support of (PA-CuO)/PSf contained long, finger-like voids that extended from the top to the bottom of the substrate cross-section which is characteristic of polysulfone membrane synthesized by the phase-inversion method.

AFM (Fig. 6) were obtained in order to compare the surface morphologies of the modified membrane ((PA-CuO)/PSf) with respect to the pristine membrane (PA/PSf). The images show that the top surfaces of the membranes exhibit characteristics consistent with those of interfacially polymerized PA membranes, which consist of ridge-and-valley layer [36]. The 2D image of modified membrane (Fig. 6c) shows similar surface features compared to the respective SEM-FE image. This fact allowed to confirm the tightly packed globular structure underneath the

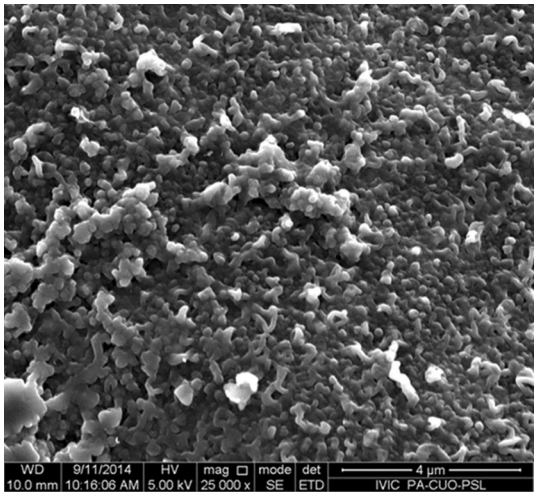

Fig. 3 Field emission microscope image (FE-SEM) of the membrane surface

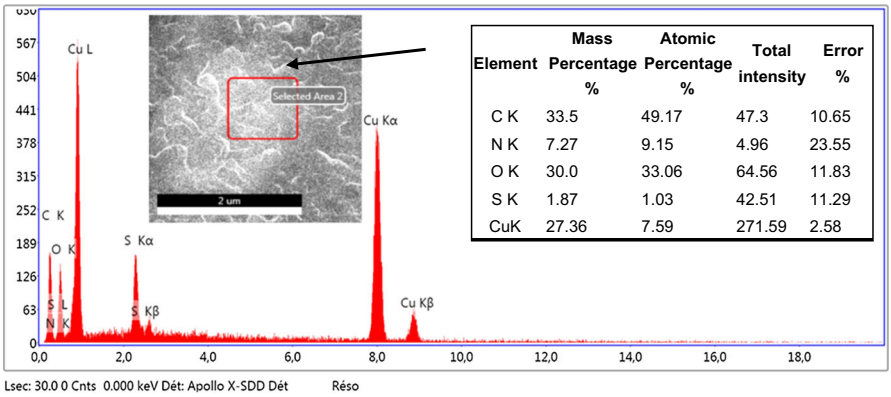

Element	Mass Percentage %	Atomic Percentage %	Total intensity	Error %
C K	33.5	49.17	47.3	10.65
N K	7.27	9.15	4.96	23.55
O K	30.0	33.06	64.56	11.83
S K	1.87	1.03	42.51	11.29
CuK	27.36	7.59	271.59	2.58

Fig. 4 EDX analysis of the (PA-CuO)/PSf membrane

ridge-and-valley layer. Furthermore, remarkable changes in the surface roughness of the membranes are clearly observed in the modified membrane (Fig. 6b) in comparison with unmodified membrane (Fig. 6a).

The root mean square roughness parameter has been increased for modified membrane with respect to unmodified membrane (Table 1). The incorporation of CuO nanoparticles (∼50 nm) into the membrane during the interfacial polymerization process significantly affected the surface roughness. This effect can be attributed to the agglomeration of nanoparticles in the surface during the polymerization process, which could change the height between ridges and valleys of the polyamide layer increasing its surface roughness. In contrast, Ben-Sasson et al. modified RO membranes with Cu-Nps (∼34 nm) by dipping as method of modification. They showed a slight increase (∼10 nm) in the root mean square roughness of the modified membranes and considered that this functionalization did not affect significantly the surface roughness [20]. It indicated that the size of CuO nanoparticles and the type of modification of the polyamide layer by incorporating these nanoparticles during interfacial polymerization process are detrimental to roughness parameters. Biofoulants are more likely to be entrapped in membranes with rougher topologies [1]; therefore, this fact could influence in the antibiofouling effect.

On the order hand, the hydrophilicity of the membranes was evaluated by contact angle measurement (Table 1). Contac angles are measured by drop shape analysis of sessile drops placed over the membrane. A slight increase in contact angle is observed for the modified membrane with values of (84 ± 2)° with respect to unmodified membranes (79 ± 1)°. Thus, no significant change in the hydrophilicity of the membranes was observed with this modification. Similar results have also been reported in previous work [20].

The zeta-potential of the membranes was analyzed in order to estimate the surface charge of the membranes. At high pH, the zeta-potential was negative with a plateau around 55 mV caused by the deprotonation of functional groups on the surface of the membranes (Fig. 7). The iep, where $\zeta = 0$, was reached at a pH of

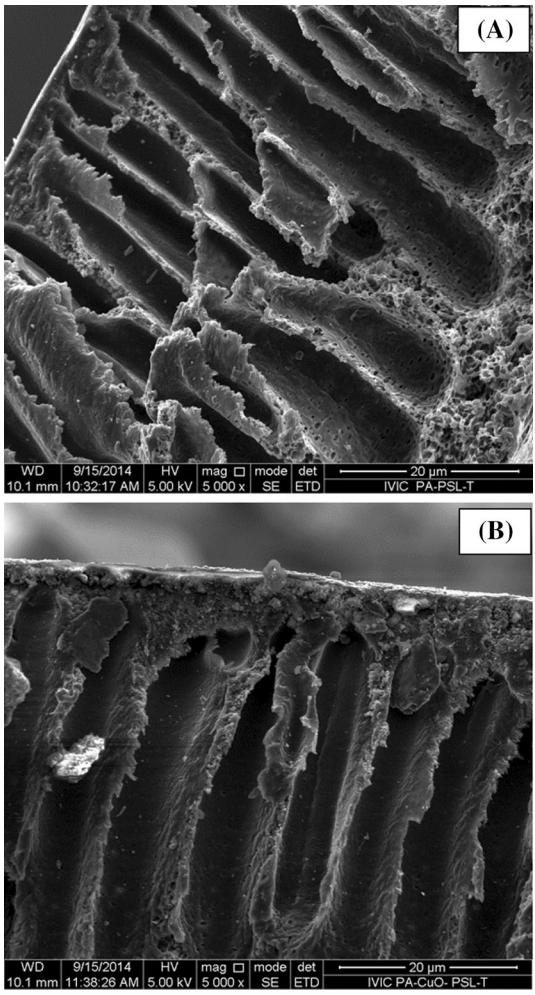

Fig. 5 Cross-section SEM of the membranes. **a** PA/PSf and **b** (PA-CuO)/PSf

2.74 for pristine membranes (PA/PSf). Below this pH value, a positive ζ-potential was found, referring to the protonation of amine functional groups. TFC-membranes have a polyamide (PA) active layer composed by functional groups: carboxylic (–COOH), amino ($–NH_2$) and amide groups [37]. In an aqueous medium (slightly acidic/alkaline) the carboxyl groups (–COOH) dissociate and become negatively charged (COO^-) producing a negative zeta-potential on surfaces [38, 39]. Introduction of nanoparticles was proven by the variation of the ζ-potential. At high pH, the lower the (negative) zeta-potential since fewer functional groups at the surface of the membrane could be deprotonated. This behavior was also observed to TFC membranes modified with alkoxysilanes [39]. Furthermore, the iep was increased from 2.74 for (PA/PSf) to 3.42 for (PA-CuO)/PSf. It has been reported that increasing the number of amino groups on the surface results in shifting the iep towards higher pH [39].

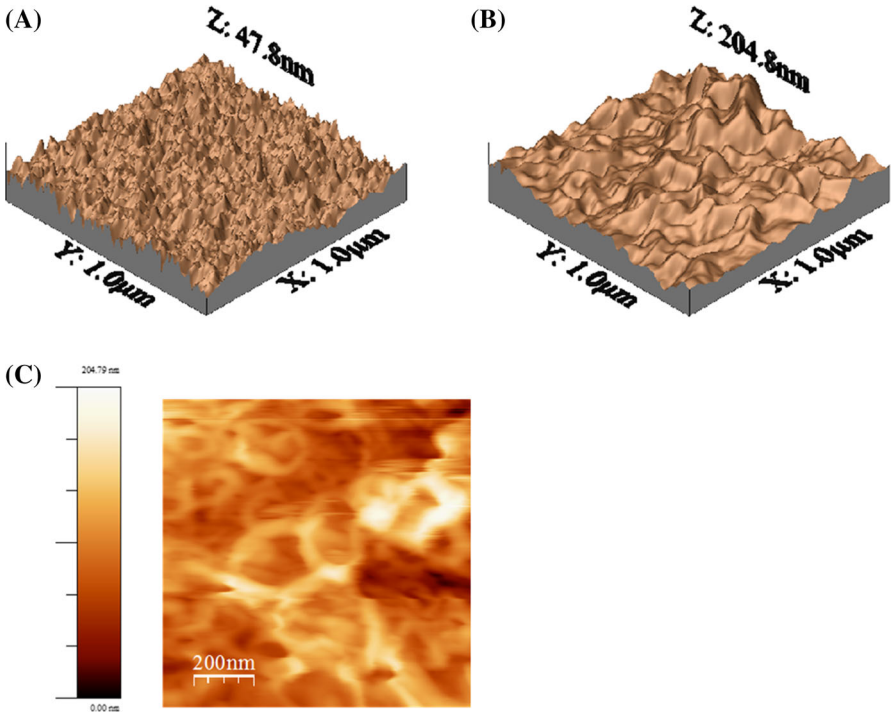

Fig. 6 AFM scan of the membranes. **a** PA/PSf, **b** (PA-CuO)/PSf, **c** 2D image of (PA-CuO)/PSf

Table 1 Surface properties of the membranes

Membrane	Root Mean Square roughness (RMS) (nm)	Contact angle (°)
PA/PSf	18 ± 4	79° ± 1
(PA-CuO)/PSf	103 ± 9	84° ± 2

These results suggest that at high pH the incorporation of CuO nanoparticles into polyamide layer during the interfacial polymerization process maintains an active polymeric layer with negative surface charge but with fewer deprotonated groups available on membrane surface in comparison with pristine membrane.

In previous work related to RO membranes modified with Cu-Nps using dipping process, the membrane surface charge became positive after functionalization attributed to the coverage of the membrane surface by positively charged Cu-NPs [20].

Thus, despite our modified membrane has an absolute value of zeta-potential lower than that of the pristine membrane, it remains a negative surface charge at the active polymeric layer.

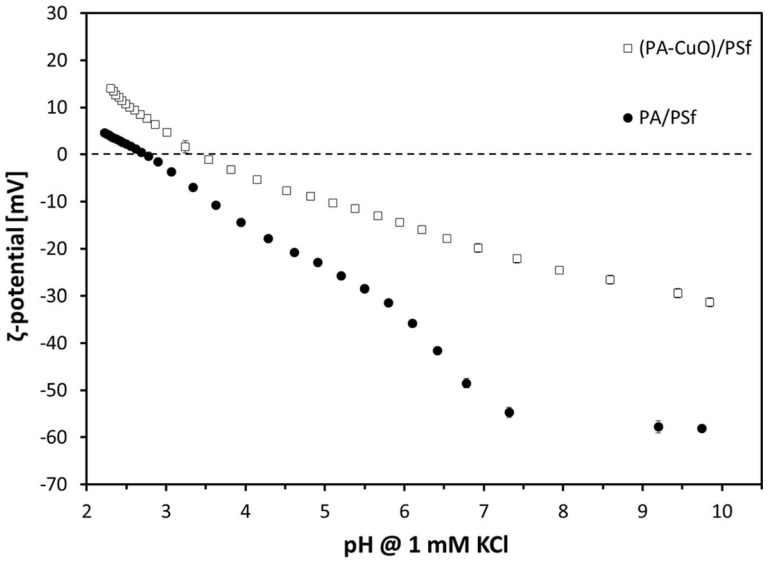

Fig. 7 Zeta potential on membranes surface

Negative surface charge favor the anti-adhesion property of the membranes as *E. coli* carry a negative cell surface charge for favoring the electrostatic repulsion between membrane and the bacteria [40].

Antibiofouling effect

The number of *E. coli* colonies formed in the medium (CFU) in presence of modified membrane ((PA-CuO)/PSf) decreased in comparison with pristine membrane (Fig. 8), demonstrating an important bactericidal effect by the modification.

Moreover, the numbers of bacteria adhering to the modified membrane (cells per mm^2) were significantly lower with respect to unmodified membrane (Fig. 9) demonstrating an excellent anti-adhesion capacity of the modified membrane.

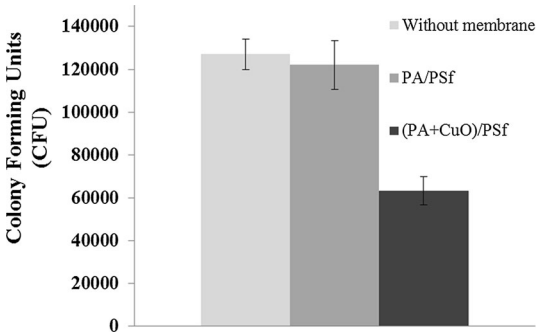

Fig. 8 Bactericidal effect of the membranes on *E. coli*

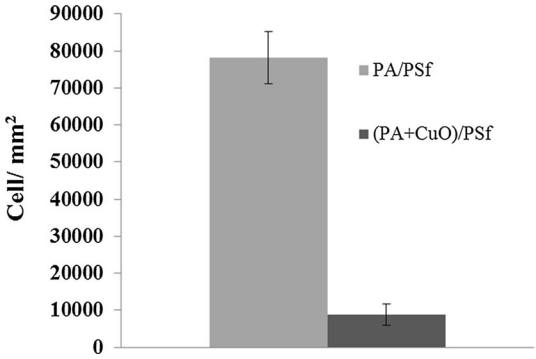

Fig. 9 Cells of *E. coli* per area of the membranes

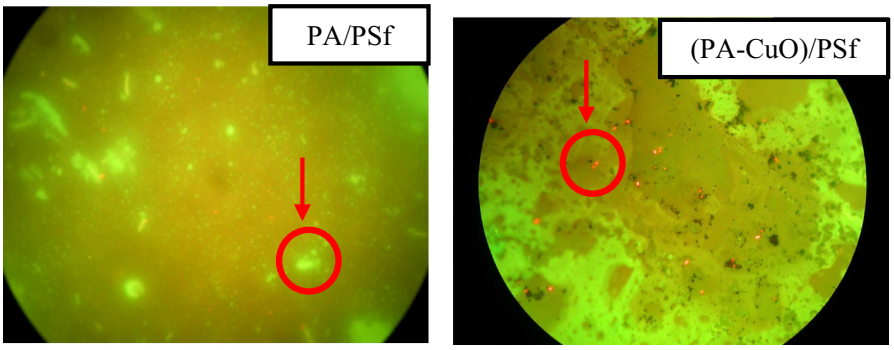

Fig. 10 Images of distribution of *E. coli* (live and dead) on the membranes by epifluorescence microscopy

Moreover, it can be noted that the little amount of bacteria adhered on the modified membrane were observed predominantly as dead bacterial (red spots) on the surface (Fig. 10).

In general, an excellent anti-adhesion capacity and significant bactericidal effect were observed in the presence of the modified membrane. This beneficial influence can be attributed to the effects generated by incorporation of CuO nanoparticles.

Bactericidal and anti-adhesion effects can be mainly attributed to the copper toxicity due to the possible release of Cu^{+2} ions from the surface of the modified membranes, given CuO is a highly ionic nanoparticle metal oxide [12, 17], releasing ion biocide into the boundary layer above the membrane to form an inhibition zone [5, 20, 41]. The Cu^{+2} ions released from the nanoparticles have a toxic effect on bacteria in the medium, because the ions trigger the production of reactive oxygen species, which damage the DNA of the bacteria killing them [42].

The reduction of number of colonies forming units (CFU) in the aqueous medium in this inhibition zone decreases the number of bacteria that could potentially attach to the membrane surface [19]. Moreover, the little amount of bacteria adhered can be susceptible to the killing by the toxic copper release into boundary layer above the membrane.

Finally, despite no favorable changes on the surface physicochemical properties of modified membranes with respect to unmodified membrane were observed (similar contact angle, higher surface roughness and less negatively charged surface), it could be noted that the modification maintains the negative surface charge of the membranes just as for the pristine membrane. This fact underlines the anti-adhesion effect of these membranes considering that material surface negatively charged can reduce the possibility of bacterial adhesion and delay the formation of a biofilm attributed to electrostatic repulsion [43].

Desalination performance

The desalination performance of modified membranes was quantified by a salt rejection of about 97% with stable water flux during 60 min and a recovery of 50%.

The flux permeate of modified membrane increases in comparison with pristine membrane (Table 2). These results demonstrate that improvement in the water flux with the incorporation of CuO nanoparticles is reached and it can be attributed to the hydrophilicity of these nanoparticles. A similar effect was observed in vacuum membrane distillation (MD) modified with CuO nanoparticles, which showed that these hydrophilic nanoparticles have a great potential to improve the performance of these membranes in terms of water flux [22].

(PA-CuO)/PSf membrane showed ~ 2 times higher flux with respect to unmodified membrane and similar salt rejection percentage was observed. Water molecules appear to flow preferentially through the hydrophilic nanoparticle, while solute rejection remains comparable to unmodified membrane. This behavior has also been observed by modified membranes by incorporating hydrophilic nanoparticles [44–46].

Conclusions

The modification of TFC-RO membrane by incorporating CuO nanoparticles in the PA layer during the interfacial polymerization process ((PA-CuO)/PSf) resulted in a potential alternative method to produce membranes with antibiofouling properties.

Significant bactericidal and excellent anti-adhesion capacities were reached. This was mainly attributed to the copper toxicity. Possible release of Cu^{+2} ions from the surface of the modified membranes into a boundary layer above the membrane forms an inhibition zone which decreases the number of bacteria that could

Table 2 Permeate flux and rejection of salts percentage of the membranes

Membrane	Flux permeate (L m^{-2} h^{-1} bar^{-1})	Rejection of salts percentage (%)
PA/PSf	1.21 ± 0.13	96.9 ± 0.2
(PA-CuO)/PSf	2.18 ± 0.64	97.4 ± 0.7

potentially attach to the membrane surface. Moreover, the little amount of bacteria adhered can be susceptible to the killing by the toxic copper release into boundary layer above the membrane.

Unfavorable changes on the surface physicochemical properties of modified membrane were observed (similar contact angle, higher surface roughness and less negatively charged surface)', however, modified membrane remained the negative surface charge of these type of membranes which underline the anti-adhesion effect by electrostatic repulsion.

The desalination performance of modified membranes was good with a salt rejection of about 97% with a stable maximum water flux about 2.18 L m^{-2} h^{-1} bar^{-1} and a recovery of 50%.

Thus, the incorporation CuO nanoparticles into TFC-RO membranes improved the antibiofouling capacities without impairing the desalination performance of the membrane. However, despite these significant findings new research challenges are needed in further study. For example, these capacities can be evaluated using gram-positive bacteria. In addition, the formation of biofouling in situ during long times of operation can be analyzed in order to evaluate the lifetime of the membrane with maintaining the anti-biofouling property.

Acknowledgements The authors gratefully acknowledge financial support provided by National Fund for Scientific and Technological Development (FONDECYT) of the Government of Chile (Project No. 11130251). The authors thank Solvay Advanced Polymers for donating the polysulfone Udel P-1700. The authors also thank the Water Quality Laboratory of the Department of Civil Engineering of Universidad de Chile for giving the infrastructure, Professor Marcos Flores of the Department of Physics of Universidad de Chile for making of AFM analyses and Surface Laboratory of Pontificia Universidad Catolica de Chile for making the contact angle measures.

References

1. Kang GD, Cao YM (2012) Development of antifouling reverse osmosis membranes for water treatment: a review. Water Res 46(3):584–600
2. Buonomenna MG (2013) Nano-enhanced reverse osmosis membranes. Desalination 314:73–88
3. Yin J, Deng B (2015) Polymer-matrix nanocomposite membranes for water treatment. J Membr Sci 479:256–275
4. Efome JE, Baghbanzadeh M, Rana D, Matsuura T, Lan CQ (2015) Effects of superhydrophobic SiO_2 nanoparticles on the performance of PVDF flat sheet membranes for vacuum membrane distillation. Desalination 373:47–57
5. Karkhanechi H, Razi F, Sawada I, Takagi R, Ohmukai Y, Matsuyama H (2013) Improvement of antibiofouling performance of a reverse osmosis membrane through biocide release and adhesion resistance. Sep Purif Technol 105:106–113
6. Ghosh AK, Bindal RC, Prabhakar S, Tewari PK (2011) Composite polyamide reverse osmosis (RO) membranes—recent developments and future directions. Technol Dev 321:43–51
7. Kango S, Kalia S, Celli A, Njuguna J, Habibi Y, Kumar R (2013) Surface modification of inorganic nanoparticles for development of organic–inorganic nanocomposites—a review. Prog Polym Sci 38(8):1232–1261
8. Kim J, Van der Bruggen B (2010) The use of nanoparticles in polymeric and ceramic membrane structures: review of manufacturing procedures and performance improvement for water treatment. Environ Pollut 158(7):2335–2349
9. Misdan N, Ismail AF, Hilal N (2016) Recent advances in the development of (bio)fouling resistant thin film composite membranes for desalination. Desalination 380:105–111

10. Cioffi N, Torsi L, Ditaranto N, Tantillo G, Ghibelli L, Sabbatini L et al (2005) Copper nanoparticle/polymer composites with antifungal and bacteriostatic properties. Chem Mater 17(21):5255–5262
11. Chapman JS (2003) Biocide resistance mechanisms. Int Biodeterior Biodegrad 51(2):133–138
12. Bagchi B, Dey S, Bhandary S, Das S, Bhattacharya A, Basu R et al (2012) Antimicrobial efficacy and biocompatibility study of copper nanoparticle adsorbed mullite aggregates. Mater Sci Eng C 32(7):1897–1905
13. Xu J, Feng X, Chen P, Gao C (2012) Development of an antibacterial copper (II)-chelated polyacrylonitrile ultrafiltration membrane. J Membr Sci 413–414:62–69
14. Asapu S, Pant S, Gruden CL, Escobar IC (2014) An investigation of low biofouling copper-charged membranes for desalination. Desalination 338:17–25
15. Hausman R, Gullinkala T, Escobar IC (2009) Development of low-biofouling polypropylene feedspacers for reverse osmosis. J Appl Polym Sci 114(5):3068–3073
16. Hausman R, Gullinkala T, Escobar IC (2010) Development of copper-charged polypropylene feedspacers for biofouling control. J Membr Sci 358(1–2):114–121
17. Akar N, Asar B, Dizge N, Koyuncu I (2013) Investigation of characterization and biofouling properties of PES membrane containing selenium and copper nanoparticles. J Membr Sci 437:216–226
18. Isloor AM, Ganesh BM, Isloor SM, Ismail AF, Nagaraj HS, Pattabi M (2013) Studies on copper coated polysulfone/modified poly isobutylene alt-maleic anhydride blend membrane and its antibiofouling property. Desalination 308:82–88
19. Karkhanechi H, Takagi R, Ohmukai Y, Matsuyama H (2013) Enhancing the antibiofouling performance of RO membranes using $Cu(OH)_2$ as an antibacterial agent. Desalination 325:40–47
20. Ben-Sasson M, Zodrow KR, Genggeng Q, Kang Y, Giannelis EP, Elimelech M (2014) Surface functionalization of thin-film composite membranes with copper nanoparticles for antimicrobial surface properties. Environ Sci Technol 48(1):384–393
21. Ben-Sasson M, Lu X, Nejati S, Jaramillo H, Elimelech M (2016) In situ surface functionalization of reverse osmosis membranes with biocidal copper nanoparticles. Desalination 388:1–8
22. Baghbanzadeh M, Rana D, Matsuura T, Lan CQ (2015) Effects of hydrophilic CuO nanoparticles on properties and performance of PVDF VMD membranes. Desalination 369:75–84
23. Ren G, Hu D, Cheng EW, Vargas-Reus MA, Reip P, Allaker RP (2009) Characterisation of copper oxide nanoparticles for antimicrobial applications. Int J Antimicrob Agents 33(6):587–590
24. Baek YW, An YJ (2011) Microbial toxicity of metal oxide nanoparticles (CuO, NiO, ZnO, and Sb_2O_3) to *Escherichia coli*, *Bacillus subtilis*, and *Streptococcus aureus*. Sci Total Environ 409(8):1603–1608
25. Aruoja V, Dubourguier HC, Kasemets K, Kahru A (2009) Toxicity of nanoparticles of CuO, ZnO and TiO_2 to microalgae *Pseudokirchneriella subcapitata*. Sci Total Environ 407(4):1461–1468
26. Shaffiey SF, Shapoori M, Bozorgnia A, Ahmadi M (2014) Synthesis and evaluation of bactericidal properties of CuO nanoparticles against *Aeromonas hydrophila*. Nanomed J 1(3):198–204
27. García A, Quintero Y, Vicencio N, Rodríguez B, Ozturk D, Mosquera E et al (2016) Influence of TiO_2 nanostructures on anti-adhesion and photoinduced bactericidal properties of thin film composite membranes. RSC Adv 6(86):82941–82948
28. Saleh TA, Gupta VK (2012) Synthesis and characterization of alumina nano-particles polyamide membrane with enhanced flux rejection performance. Sep Purif Technol 89:245–251
29. Zhang M, Zhang K, De Gusseme B, Verstraete W (2012) Biogenic silver nanoparticles (bio-Ag 0) decrease biofouling of bio-Ag 0/PES nanocomposite membranes. Water Res 46(7):2077–2087
30. Lee HS, Im SJ, Kim JH, Kim HJ, Kim JP, Min BR (2008) Polyamide thin-film nanofiltration membranes containing TiO_2 nanoparticles. Desalination 219(1–3):48–56
31. Johan MR, Suan MSM, Hawari NL, Ching HA (2011) Annealing effects on the properties of copper oxide thin films prepared by chemical deposition. Int J Electrochem Sci 6(12):6094–6104
32. Tang CY, Kwon Y-N, Leckie JO (2009) Effect of membrane chemistry and coating layer on physiochemical properties of thin film composite polyamide RO and NF membranes. Desalination 242(1–3):149–167
33. Akin O, Temelli F (2011) Probing the hydrophobicity of commercial reverse osmosis membranes produced by interfacial polymerization using contact angle, XPS, FTIR, FE-SEM and AFM. Desalination. 278(1–3):387–396
34. Silverstein RM, Webster FX, Kiemle DJ (2005) Spectrometric identification of organic compounds, 7th edn. Wiley, Hoboken
35. Porter MC (1991) Handbook of industrial membrane technology. Noyes Publications, New York

36. Kwak S-Y, Jung SG, Yoon YS, Ihm DW (1999) Details of surface features in aromatic polyamide reverse osmosis membranes characterized by scanning electron and atomic force microscopy. J Polym Sci Part B Polym Phys 37:1429–1440
37. Tang C, Kwon Y, Leckie J (2007) Probing the nano- and micro-scales of reverse osmosis membranes—a comprehensive characterization of physiochemical properties of uncoated and coated membranes by XPS, TEM, ATR-FTIR, and streaming potential measurements. J Membr Sci 287(1):146–156
38. Bauman M, Košak A, Lobnik A, Petrinić I, Luxbacher T (2013) Nanofiltration membranes modified with alkoxysilanes: surface characterization using zeta-potential. Colloids Surf A 422:110–117
39. Coronell O, Mariñas BJ, Zhang X, Cahill DG (2008) Quantification of functional groups and modeling of their ionization behavior in the active layer of FT30 reverse osmosis membrane. Environ Sci Technol 42(14):5260–5266
40. Gilbert P, Evans DJ, Evans E, Duguid IG, Brown MRW (1991) Surface characteristics and adhesion of *Escherichia coli* and *Staphylococcus epidermidis*. J Appl Bacteriol 71(1):72–77
41. Banerjee I, Pangule RC, Kane RS (2011) Antifouling coatings: recent developments in the design of surfaces that prevent fouling by proteins, bacteria, and marine organisms. Adv Mater 23(6):690–718
42. Bondarenko O, Ivask A, Kakinen A, Kahru A (2012) Sub-toxic effects of CuO nanoparticles on bacteria: kinetics, role of Cu ions and possible mechanisms of action. Environ Pollut 169:81–89
43. Gottenbos B, Grijpma DW, van der Mei HC, Feijen J, Busscher HJ (2001) Antimicrobial effects of positively charged surfaces on adhering Gram-positive and Gram-negative bacteria. J Antimicrob Chemother 48:7–13
44. Li D, Wang H (2010) Recent developments in reverse osmosis desalination membranes. J Mater Chem 20(22):4551
45. Jeong B-H, Hoek EMV, Yan Y, Subramani A, Huang X, Hurwitz G et al (2007) Interfacial polymerization of thin film nanocomposites: a new concept for reverse osmosis membranes. J Membr Sci 294(1–2):1–7
46. Lind ML, Jeong B-H, Subramani A, Huang X, Hoek EMV (2009) Effect of mobile cation on zeolite-polyamide thin film nanocomposite membranes. J Mater Res 24(05):1624–1631